DENTAL MATERIALS 29 (2013) 954–962

Available online at www.sciencedirect.com

SciVerse ScienceDirect

journal homepage: www.intl.elsevierhealth.com/journals/dema

Physico-chemical characterization of zirconia–titania composites coated with an apatite layer for dental implants

Juliana Marchi[a,*], *Eric M. Amorim*[a], *Dolores R.R. Lazar*[b], *Valter Ussui*[b], *Ana Helena A. Bressiani*[b], *Paulo Francisco Cesar*[c]

[a] *Centro de Ciências Naturais e Humanas, Universidade Federal do ABC, Santo André, SP, Brazil*
[b] *Centro de Ciência e Tecnologia de Materiais, Instituto de Pesquisas Energéticas e Nucleares, São Paulo, SP, Brazil*
[c] *Departamento de Biomateriais e Biologia Oral, Faculdade de Odontologia, Universidade de São Paulo, São Paulo, SP, Brazil*

ARTICLE INFO

Article history:
Received 18 September 2012
Received in revised form 7 June 2013
Accepted 2 July 2013

Keywords:
Dental implant
Ceramic composite
Y-TZP
Titania
Biomimetic coating

ABSTRACT

Objectives. To investigate the crystalline phases, morphological features and functional groups on the surface of sintered Y:TZP/TiO_2 composite ceramics before and after the application of a biomimetic bone-like apatite layer. The effect of TiO_2 content on the composite's characteristics was also evaluated.

Methods. Samples of Y:TZP containing 0–30 mol% TiO_2 were synthesized by co-precipitation, followed by filtration, drying and calcination. The powders were uniaxially pressed and sintered at 1500 °C/1 h. To obtain biomimetic coatings the samples were exposed to sodium silicate solution and then to a concentrated simulated body fluid solution. The surfaces, before and after coating, were characterized by diffuse reflectance infrared Fourier transformed spectroscopy, X-ray diffraction analysis and scanning electron microscopy.

Results. The surfaces of all Y:TZP/TiO_2 samples were covered with a dense and uniform calcium phosphate layer with a globular microstructure. This layer was crystalline for specimens with 30% of TiO_2 and amorphous for specimens with 0 and 10% of TiO_2. Chemical analysis indicated that this layer was composed of type A carbonate apatite. Among the materials tested, the composite with 10% of TiO_2 showed the best overall chemical and physical features, such as higher density and more cohesive amorphous apatite layer.

Significance. Y-TZP-based materials obtained in the present investigation by means of the successful association of a calcium phosphate biomimetic layer with small amounts TiO_2 should be further explored as an option for ceramic dental implants with improved bioactivity.

* *Corresponding author at*: CCNH/UFABC, Rua Santa Adélia, 166, Bangu, 09210-170 Santo André, SP, Brazil. Tel.: +55 11 4996 7960; fax: +55 11 4996 0090.
E-mail addresses: juliana.marchi@ufabc.edu.br, juliana.marchi@hotmail.com (J. Marchi).
0109-5641/$ – see front matter
http://dx.doi.org/10.1016/j.dental.2013.07.002

1. Introduction

Substituting commercially pure titanium or titanium alloys (*e.g.*, Ti–6Al–4V) for dental implants is one of the biggest challenges faced by biomaterials scientists nowadays. Titanium based implants have well recognized advantages like excellent osteointegration demonstrated by the high levels of bone-to-implant contact reported in clinical studies [1,2], and the high fracture toughness typically found in metallic alloys which guarantees low fracture rates.

The highly biocompatible behavior of titanium implants is associated to the corrosion resistance of the passivation oxide layer. Although this layer is very homogenous and strongly bonded to the implant surface, allergenic responses have been associated to the use of titanium dental implants [3] and biocompatibility tests have demonstrated that ceramic materials like alumina or zirconia are significantly more biocompatible than titanium alloys [4,5].

Due to their high biocompatibility, ceramic materials like yttria stabilized tetragonal zirconia polycrystals (Y-TZP) have been the focus of many studies and are proposed as important candidates to substitute titanium implants. The main drawback related to the use of ceramic materials in structural biomedical applications is their relatively low fracture toughness (K_{Ic}), especially when compared to metals. However, because of the its intrinsic martensitic transformation toughening mechanism, and the compressive stresses associated to it, Y-TZP ($K_{Ic} = 9.0\,MPa\,m^{1/2}$) is currently commercialized as a substitute for metallic implants since it has sufficient mechanical properties to withstand the stresses found in the oral cavity. In addition, Y-TZP is a white material, and therefore can partially overcome the poor esthetic results associated to metal structures when in contact with gingival tissues.

Two key issues still need to be addressed with regards to the use of Y-TZP for dental implants: low temperature degradation (LTD) and bioinertness. LTD, also known as "aging", was initially observed on the surface of Y-TZP femoral head implants that underwent water-assisted martensitic transformation with subsequent increase in roughness and nucleation/growth of cracks toward the bulk of the material [6]. Further clinical research is still necessary to understand the implications of LTD in the clinical use of Y-TZP dental implants [7].

Bionertness can be defined as the lack of interaction between the Y-TZP surface and the surrounding living tissues [8,9] The poor bioactivity of these ceramics usually leads to problems in the osteointegration process, as it hinders the cellular response in terms of proliferation, migration and adhesion [10] and can ultimately cause implant failure due to formation of a fibrous capsule around the artificial root [11,12]. Hence, surface modification of Y-TZP dental implants can be an important procedure to improve the final clinical results in terms of osteointegration.

Surface modification of Y-TZP surfaces for biomedical purposes is currently performed by material subtraction or addition of bioactive layers. Removing material from the implant surface can cause leaching of ytria, undesirable phase transformations, and nucleation of critical surface flaws [13]. On the other hand, both good osteoinegration results and faster bone regeneration have been reported after the addition of bioceramic layers to Y-TZP implants, such as calcium phosphate or bioactive glass [14]. These additive approaches also present disadvantages like adhesion problems between the layer and the implant and heterogeneity of the applied film [13].

Another approach that aims at solving the problem of bioinertness in zirconia-based implants is the development of new composite ceramics by adding bioactive materials to a zirconia matrix. In a previous study [15], our research group has successfully developed a novel composite for implant applications by combining ZrO_2 and TiO_2. The idea behind the creation of this material was to take advantage of the good mechanical properties of ZrO_2 and the bioactivity of TiO_2 ceramics. Fortunately these two materials can be combined to form a composite due to the high solid solubility of the original oxides.

ZrO_2–TiO_2 has been successfully used in other applications as catalysts, dielectric materials, and photosensitive cells [16,17]. However, our initial study on ZrO_2–TiO_2 sintered ceramic was the first to propose this specific material for biological applications. It was demonstrated that the surfaces of samples containing both zirconia and titania had better proliferation results after cell culture experiments compared to pure zirconia or titania. Moreover, others [18,19] have showed that the presence of TiO_2 induced *in vitro* bone-like apatite formation and stimulated osteoconductivity *in vivo*.

In the present study, our aim was to improve the previously developed ZrO_2–TiO_2 composite by adding a bioactive/biomimetic bone-like apatite layer. This type of layer can improve osteointegration and has been successfully applied to coat other bioceramics such as silicon nitride and alumina–zirconia composites [20,21]. However, its use to functionalize ZrO_2–TiO_2 biocomposites has not been explored yet. Apatite thin films can be produced in acellular simulated body fluids (SBF) with ionic composition similar to that of the inorganic part of human blood plasma [22]. After immersion of the ceramic surface in a concentrated simulated body fluid (1.5 SBF), the sodium silicate solution acts as a nucleating agent [23]. This treatment creates several calcium phosphate precursor sites on the ceramic surface, which eventually create a suitable condition for nucleation and growth of calcium phosphate phases.

The objective of this investigation was to compare the crystalline phases, morphological features and functional groups found on the surface of sintered Y:TZP/TiO_2 composite ceramics before and after the application of a biomimetic bone-like apatite layer. The effect of TiO_2 content (from 0 to 30%) on the aforementioned characteristics of the ceramic composite was also assessed. The main hypothesis of the study was that the addition of biomimetic layer to the Y:TZP/TiO_2 composite would result in a surface layer with morphological and physicochemical properties that are significantly better than those of their non-layered counterparts from the biological standpoint, *i.e.*, the presence of a TiO_2 and calcium phosphate bioactive layer with globular aspect, which is expected to favor the osteointegration process.

Table 1 – Composition of Y:TZP/TiO_2 powder mixtures and theoretical density (TD).

Sample	Composition (mol%)			TD (g/cm^3)
	ZrO_2	Y_2O_3	TiO_2	
Z	97	3	0	6.01
Z T10	87.3	2.7	10	5.77
Z T30	67.9	2.1	30	5.34

2. Materials and methods

2.1. Powder synthesis

The synthesis of Y:TZP/TiO_2 powders was described in our previous paper [24]. Briefly, zirconium oxchloride, titanium chloride and ytttrium chloride solutions were prepared to obtain different amounts of TiO_2 in the Y:TZP/TiO_2 composites (Table 1). The suspensions were filtered, washed with water, ethanol and n-butanol. After azeotropic distillation, the Y:TZP/TiO_2 ceramic powders were dried at 100 °C calcined (800 °C/1 h, Fornitec), and milled in a high energy attrition mill for 24 h using zirconia ball media in ethyl alcohol.

2.2. Powder characterization

Ceramic powders were classified with different sieves (60, 150, 270, and 325 Mesh/Tyler). The specific surface area was determined using the N_2 gas adsorption method. N_2 gas molecules were adsorbed on the surfaces of the samples and the surface area of the powder calculated by the BET (Brunauer, Emmet and Tellller) method. The mean diameters of the particles were estimated using Eq. (1).

$$S_{BET} = \frac{6}{\rho_m D} \quad (1)$$

where S_{BET} is the specific surface area, ρ_m is the theoretical density of the mixtures and D is the mean particle diameter.

The crystalline phases of the Y:TZP/TiO_2 powders were identified from X-ray powder diffraction profiles (XRD, Rigaku DMAX 3000 diffractometer, Cu Kα). The diffraction profiles were compared with files of the International Centre for Diffraction Data (ICDD) for standard phases 037-1484, 081-1545 and 034-0415, corresponding to monoclinic zirconium dioxide (ZrO_2), tetragonal zirconium dioxide (ZrO_2) and zirconium titanate ($ZrTiO_4$) phases, respectively. The morphological features of the powders were examined in a scanning electron microscope with a field emission gun (SEM-FEG).

2.3. Y:TZP/TiO_2 samples processing

The milled and homogenized powder mixtures were dried at 90 °C and uniaxially pressed at 50 MPa using cylindrical metallic dies (6 mm in diameter), that resulted in pellets ~4 mm high. Ten samples of each composition were prepared. The samples were then sintered at 1500 °C for 60 min in a furnace (Lindberg Blue). The sample surfaces were rectified using a diamond-encrusted drill (D-91, Winter).

2.4. Samples characterization

Density measurements were performed using the geometric method and the final densities of the samples were expressed in terms of the theoretical density of each mixture. The theoretical densities of all powder mixtures were determined using the rule of mixtures [25] (Table 1), and considering 6.01 g/cm^3 and 4.24 g/cm^3 as the theoretical densities of Y:TZP and rutile TiO_2 [26], respectively. Ten samples of each composition were prepared. The roughness of the ceramic surfaces was measured with a portable Mitutoyo Surftest 211 roughmeter. Mean roughness (Ra) was estimated using the mean value of three different parallel oriented values. Densities and roughness data were estimated considering the mean and standard deviation of the ten individual measurements for each composition, which were further compared by analysis of variance (ANOVA) with a 5%level of significance ($p \leq 0.05$).

The sintered samples were analyzed using x ray powder diffraction analysis (XRD, Rigaku DMAX 3000 diffractometer, Cu Kα) to identify the crystalline phases. To observe the crystal shapes and grain sizes as well as their distribution, a scanning electron microscope (SEM, XL 30, Philips) was used, considering at least two samples for each composition.

Superficial functional groups of the sintered samples (two samples for each composition) were analyzed by diffuse reflectance infrared Fourier transformed (DRIFT) spectroscopy (Thermo Nicolet, Nexus 400) between 400 and 4000 cm^{-1}.

2.5. Biomimetic experimental method

2.5.1. Coating procedure

The Y:TZP/TiO_2 samples (five for each group) were coated with a calcium phosphate phase using the biomimetic method, as described in our earlier work [20]. Briefly, samples were immersed in sodium silicate solution for seven days, washed in deionized water, dried at room temperature, and immersed in 1.5 SBF for seven days. The solution was changed every two days. After the coating procedure, the Y:TZP/TiO_2 samples were washed and dried. All coating procedures were performed in a shaker at 40 rpm at 36.5 °C (TE-420, Tecnal).

2.5.2. Characterization of coated Y:TZP/TiO_2 samples

After coating, the surfaces of the samples were characterized by X-ray diffraction analysis (Rigaku DMAX 2000 difratometer), scanning electron microscopy (Philips, XL30) and diffuse reflectance infrared Fourier transformed spectroscopy (DRIFT, Thermo Nicolet, Nexus 400). Two specimens were used for each analysis.

3. Results

3.1. Powder characterization

Specific surface area (S BET) and mean particle size (D med) of Y:TZP/TiO_2 powders are shown in Table 2. All powders presented specific surface area higher than 39 m^2/g and are in the nanoscale range, with the estimated mean particle size lower than 27 nm. As the surface area increases, there is a decrease in mean particle size. However, no correlation can

Table 2 – Specific surface area and mean particle diameter of Y:TZP/TiO_2 powders.

Sample	S_{BET} (m^2/g)	Dm (nm)
Z	49.0	20.4
Z T10	39.1	26.6
Z T30	46.1	24.4

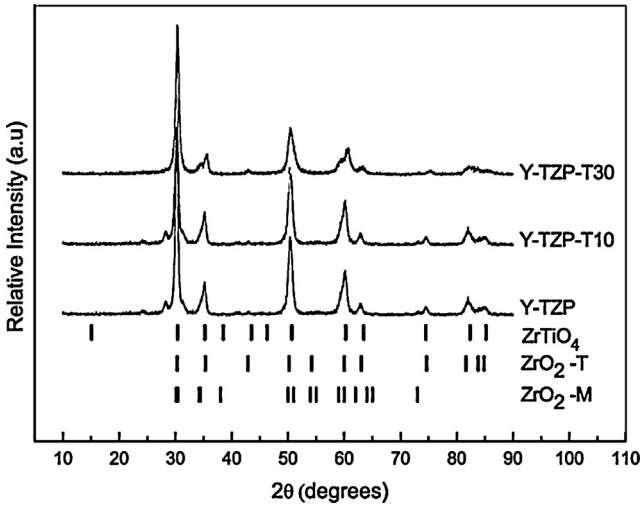

Fig. 1 – X-ray diffraction patterns of Y:TZP/TiO_2 powders.

be seen between the amount of TiO_2 in Y:TZP/TiO_2 powders and these powders features.

X-ray diffraction profiles of Y:TZP/TiO_2 powders are shown in Fig. 1. Both tetragonal and monoclinic phases of zirconium dioxide (ZrO_2) were identified in all powders. As the TiO_2 amount increased, the monoclinic phase decreased. Moreover, in sample ZT30, a crystalline zirconium titanate ($ZrTiO_4$) phase was also detected. The formation of this phase was identified by peak division between 34° and 36°.

The scanning electron micrographs of the studied powders are shown in Fig. 2. All powders were fine, rough and homogeneously dispersed. Pure zirconia powder (Z) had the highest tendency for agglomeration (Fig. 2a) compared to Y:TZP/TiO_2 powders. As the TiO_2 amount increased, the powder mixture seemed to be less agglomerated.

3.2. *Sample characterization before coating*

Geometric densities of samples after sintering are shown in Table 3. All samples showed final densities higher than 88% td. The highest density values ($p < 0.05$) were observed for ZT10 samples. Roughness values are also shown in Table 3. A relatively high standard deviation is observed for these results, indicating no significant difference amongst them.

Table 3 – Final density (% TD) and roughness (Ra, μm) of Y:TZP/TiO_2 sintered samples ($p < 0.05$).

Sample	% TD	Ra (μm)
Z	88.0 (0.4)[a]	105 (30)
Z T10	94.1 (0.3)[b]	97 (12)
Z T30	88.9 (0.4)[a]	85 (20)

X-ray diffraction profiles of sintered ceramic samples are shown in Fig. 3a. It can be seen that the Z sample has a mixture of monoclinic and tetragonal zirconia phases. The sample with intermediary TiO_2 content (ZT10) had only tetragonal symmetry. In addtition, ZT30 had both tetragonal zirconia and zirconium titanate phases.

Scanning electron micrographs of Y:TZP/TiO_2 sample surfaces are shown in Fig. 4a–c. The surfaces of ceramics had similar overall microstructure and were irregular and relatively rough, containing grooves with varied depth, caused by the surface rectification procedure. The increase in the TiO_2 content of the Y:TZP/TiO_2 samples seemed to increase the surface irregularity, as it was possible to note superficial material detachment in Fig. 4c.

The DRIFT spectrum of the samples (Fig. 6a) revealed the presence of several functional groups on the surface of sintered Y:TZP/TiO_2 ceramics, such as stretched C—H, C—O and Me—O bond vibrations (Me = Ti or Zr). Ceramic surfaces with high TiO_2 content had C—H stretching bands. As expected, all samples revealed Zr—O bond vibration, and all Y:TZP/TiO_2 mixture samples presented Ti—O bond vibration. The TiO_2 content seemed to interfere with the band position of the CO_2 functional group (band 4 indicated in Fig. 6a), dislocating it to the left.

3.3. *Samples characterization after coating*

The X-ray diffraction profiles of the coated Y:TZP/TiO_2 samples are shown in Fig. 3b. ZrO_2 phases were identified in all samples. In sample ZT30, a crystalline zirconium titanate ($ZrTiO_4$) phase was also detected. In addition, it was possible to identify minor $Ca_4P_6O_{19}$ (ICDD 015-0177) phase in this sample, as calcium phosphate crystalline phase.

Scanning electron micrographs of sample surfaces after biomimetic coating are shown in Fig. 5. A dense and uniform calcium phosphate layer, homogeneously precipitated on the entire surface, was observed on all samples. The calcium phosphate deposited on the Z and ZT30 samples (Fig. 5a and c, respectively) seemed to be looser compared to ZT10 (Fig. 5b), which had an apparently more cohesive layer. In this figure (Fig. 5b), multiple coating layers can also be observed. The morphology and the features of the coating layer can be better seen in higher magnification (Fig. 5d–f).

The surface features of the biomimetic coated ceramics were further analyzed by DRIFT technique (Fig. 6b) and different functional groups on the surface of the ceramics were revealed. Specifically, strong band of PO_4^{-3} (585, 1010 and 1100 cm^{-1}) and weak band of CO_3^{-2} vibrations (868 and 1485 cm^{-1}) were identified. Moreover, typical bands of H_2O (1647 cm^{-1}) and OH^- (between 3000 and 3600 cm^{-1}) were also observed for all samples. As seen for sintered samples before coating, the TiO_2 content affected the band position of the CO_2 functional group (band 7 indicated in Fig. 6b).

4. Discussion

The main hypothesis of the present investigation was accepted since the physical and chemical techniques used to characterize the Y:TZP/TiO_2 bioceramic specimens

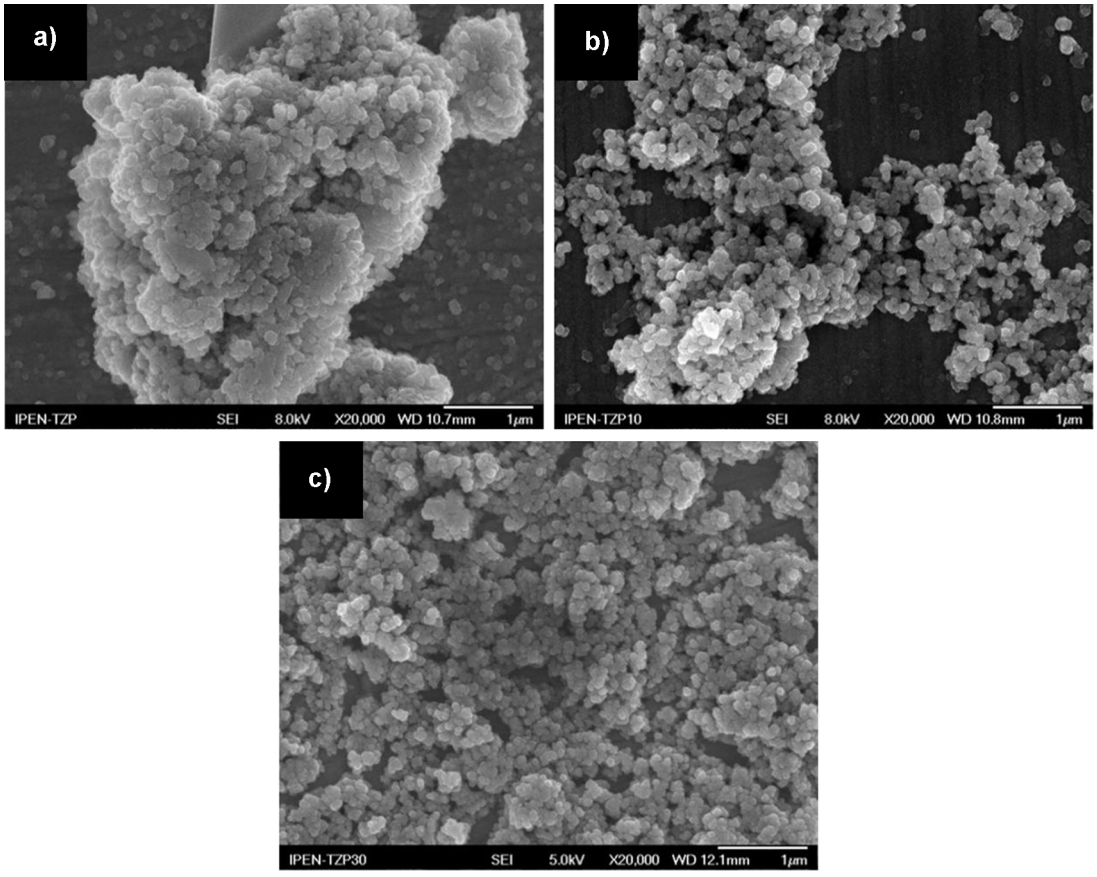

Fig. 2 – Scanning electron micrographs of Y:TZP/TiO_2 powders: (a) Z; (b) ZT10; and (c) ZT30.

indicated that their surfaces were successfully covered with a dense and uniform calcium phosphate layer with a globular microstructure, which has the potential to be highly bioactive and enhance osseointegration *in vivo*. The association of this biomimetic layer to the presence of small amounts of a more bioactive material like TiO_2 may improve the biological performance of Y:TZP-based dental implants.

The use of a biomaterial in a specific field depends on its physical and chemical properties which are affected by the synthesis procedures, surface treatments and biocompatibility, besides other features [27,28]. In a previous research work [15], we carried out cell adhesion and proliferation tests on a new sintered ZrO_2–TiO_2 ceramic composite that combined the mechanical properties of ZrO_2 with the biological characteristics of TiO_2. However, the amount of TiO_2 added to the composite was relatively high (40–60 mol%) and concerns were raised as to the negative effects it could have on the final mechanical properties of the implant component. In order to avoid this problem, the composite material used in the present study was developed

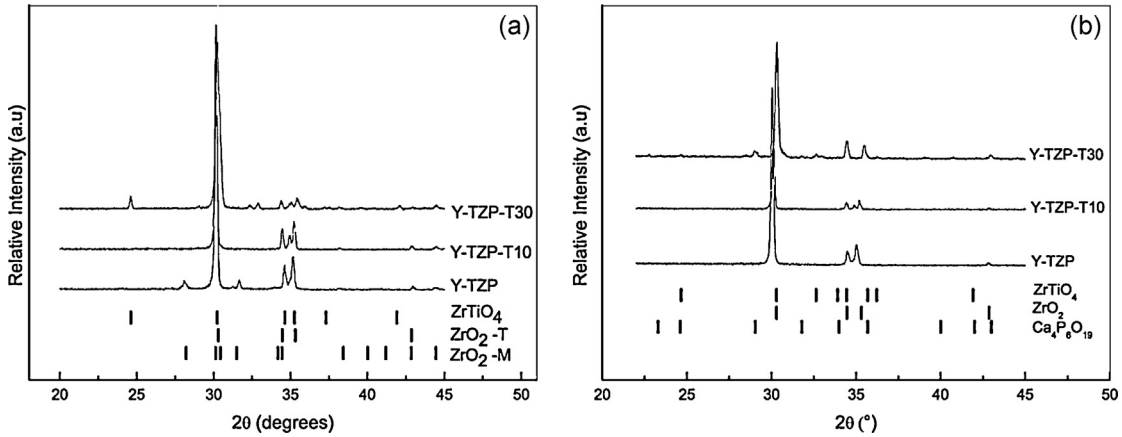

Fig. 3 – X-ray diffraction patterns of Y:TZP/TiO_2 samples after sintering at 1500 °C/1 h: (a) before coating; and (b) after coating.

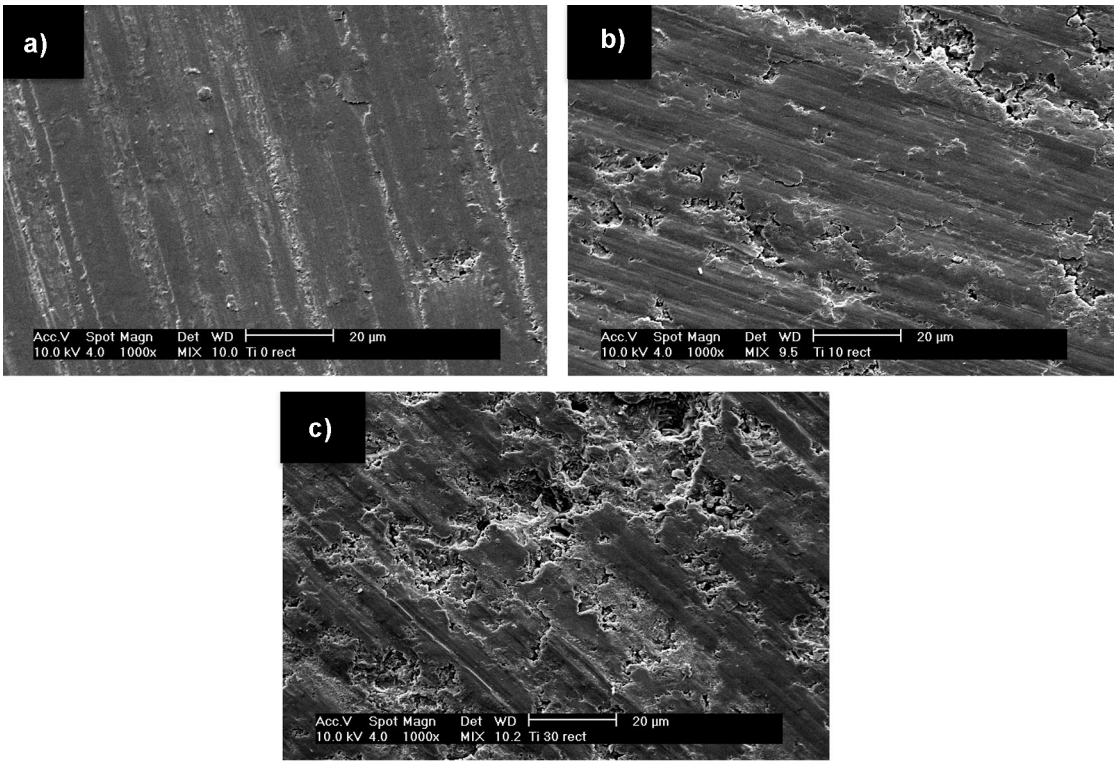

Fig. 4 – Scanning electron micrographs of Y:TZP/TiO_2 samples surface after sintering at 1500 °C/1 h, before coating: (a) Z; (b) ZT10; and (c) ZT30.

using a tougher material (Y:TZP) and lower content of TiO_2 (up to 30 mol%).

The development of the Y:TZP/TiO_2 composite started with powder characterizations of the mixtures to define the processing conditions. As shown in Section 3, all powders were fine, agglomerated and with a high specific surface area (around 45 m^2/g). These powder features indicated high reactivity, which is an important requirement for biomaterials precursors [29]. The presence of TiO_2 reduced the tendency for agglomeration of Y:TZP/TiO_2 powder mixtures. The difference between the mean particle diameter determined from the specific surface area data and the SEM examinations can be attributed to the non-spherical and rough characteristic of the powders [30].

The sintered Y:TZP/TiO_2 composites produced in this study showed relatively high final density (higher than 88%) and the ZT10 group showed significantly higher density compared to the other groups, what is a good indicator that this composition is the best option for structural implant applications. One important aspect evidenced by the DRX analysis was the presence of zirconia monoclinic phase only in the Z group, indicating that both the presence of titania and the higher density of the ZT10 and ZT30 groups avoided spontaneous martensintic transformation, resulting in better retention of the zirconia tetragonal phase. Another important surface feature noticed in the non-coated ceramic materials under the SEM was the slightly higher superficial irregularity in specimens containing titania. The lower hardness of this phase in comparison to zirconia is responsible for the material detachment observed in these specimens after the polishing procedure. Changes in the specimen polishing protocol may overcome this problem and result in smoother surfaces.

To create the biomimetic layer over the Y:TZP/TiO_2 composite, the substrate material was treated with a sodium silicate solution, to increase apatite nucleation through silanol group (Si–OH) formation. The use of a simulated body fluid solution with high ion concentration leads to faster formation of apatite and deposition of a more uniform layer [31]. The three analytical techniques (XRD, SEM and DRITF) used in this investigation complemented each other and successfully demonstrated the formation of a calcium phosphate phase after the biomimetic coating procedure. For samples with the highest TiO_2 content (ZT30), XRD analysis indicated that this calcium phosphate layer was crystalline. On the other hand, for Z and ZT10 samples the SEM and DRIFT analysis suggested that the calcium phosphate was amorphous.

DRIFT spectroscopy helped confirm the presence of $PO_4^{3-}$and CO_3^{2-} groups on the surfaces of all Y:TZP/TiO_2 ceramics after *in vitro* biomimetic procedures. These results are in agreement with those of Rey at al [32], who reported that three carbonate bands appeared in the υ_2 CO_3 domain at 878, 871 and 866 cm^{-1}. According to their results, these bands were assigned to the three different locations of the ion in the studied mineral bone and could be related to different properties of the apatite structure, such as ionic affinity for crystallographic locations and ion exchange [33]. In the present study, it is likely that due to the presence of 878 cm^{-1} CO_3^{-2} band, the carbonate ion substituted OH^- ions in the apatite structure forming a type A carbonate apatite. Moreover, the DRIFT spectra suggests that the presence of TiO_2 in a Y:TZP/TiO_2

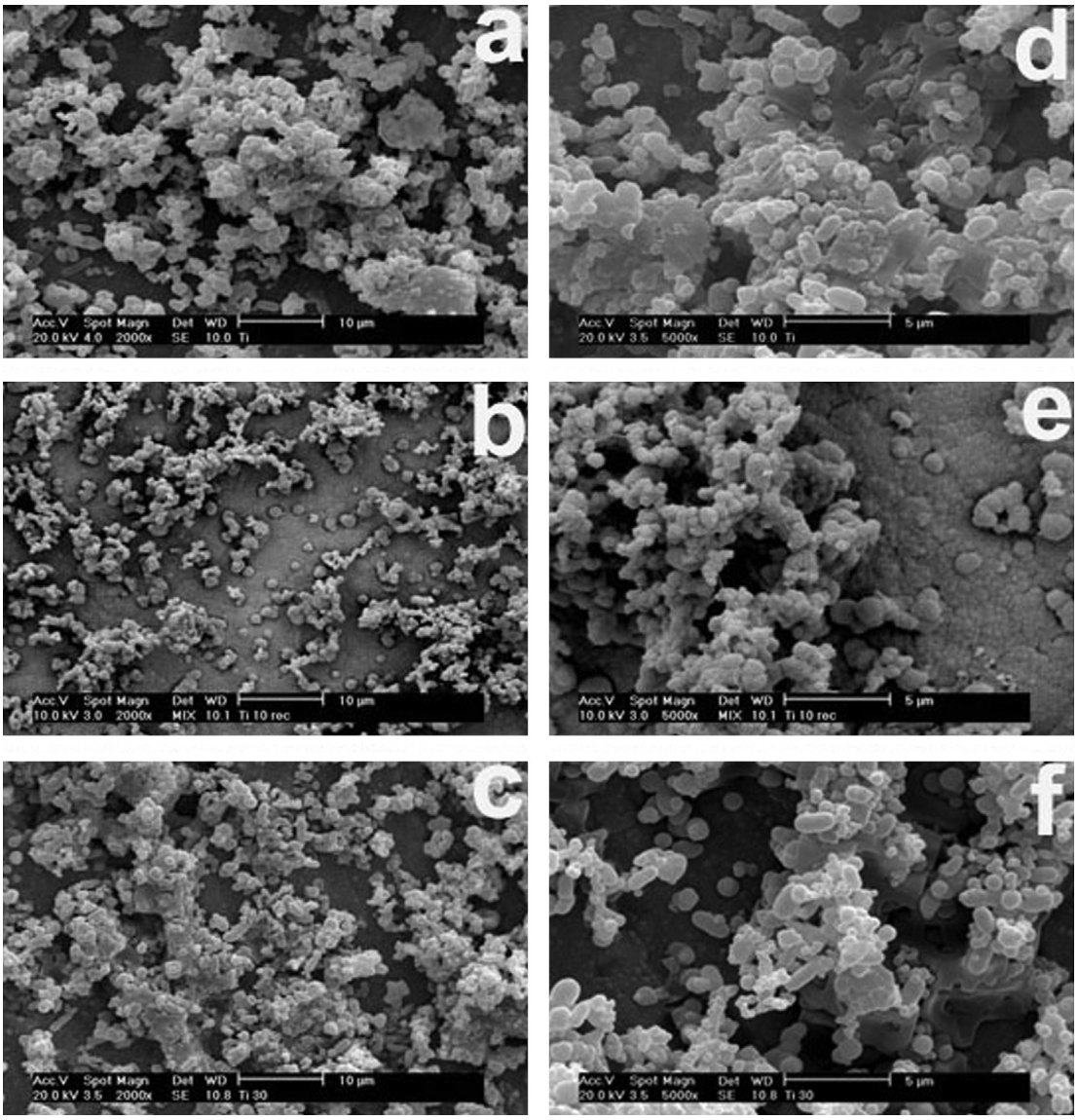

Fig. 5 – Scanning electron micrographs of Y:TZP/TiO_2 samples surface after sintering at 1500 °C/1 h, after coating, showing different magnitudes: (a) and (d) Z; (b) and (e) ZT10; (c) and (f) ZT30.

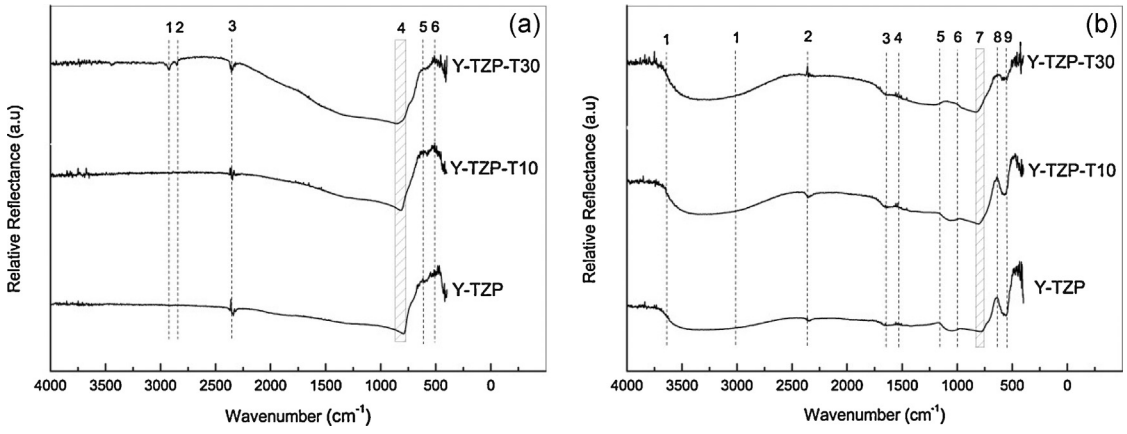

Fig. 6 – DRIFT spectra of Y:TZP/TiO_2 samples surface after sintering at 1500 °C/1 h. (a) Before coating: (1) C—H stretching (CH_3); (2) C—H stretching (CH_2); (3) C—O stretching; (4) C—O (CO_3^{-2}); (5) Ti—O bond vibration; (6) Zr—O bond vibration bond vibration; (b) after coating: (1) O—H stretching; (2) C—O stretching (CH_3); (3) O—H bending; (4) H_2O; (5) PO_4^{-3}; (6) PO_4^{-3}; (7) C—O (CO_3^{-2}); (8) PO_4^{-3}.

mixture may have affected the tendency for formation of type A or B carbonate apatite structure. It has been reported that the calcium phosphate apatite that constitutes bone mineral is a mixed AB-type substitution [34] and therefore the type A carbonate apatite formed on the specimens' surfaces is expected to have good bioactivity. Finally, the adsorption band of PO_4^{-3} observed at 625 cm^{-1} for all Y:TZP/TiO_2 biomimetic coated samples can be related to the amorphous apatite deposited on Z and Z10 surfaces. In fact, Rey et al. [35] also found a fainted band at both 620–625 cm^{-1} and 585 cm^{-1} bands in FTIR spectra of very young tissues or in freshly precipitated apatite.

The results of the current study suggest that there exists an affinity of the non-crystalline calcium phosphate precipitates for the Y:TZP/TiO_2 based ceramic substrate, what can result in good bioactive properties of the implant surface. The apatite nucleation on the sample surface is probably associated the presence Me–OH functional groups (Me = Zr or Ti) on the bioceramic. After formation of apatite nuclei, they can successfully grow upon immersion in concentrated SBF. The ZT10 samples covered with the apatite layer were considered the ones with best potential to become a successful implant material because they showed a more cohesive layer compared to ZT30, which suggests better adhesion of the layer to the implant surface. Besides, the calcium phosphate phase detected for ZT10 was amorphous as opposed the crystalline nature of the layer observed for ZT30, as confirmed by the DRX analysis. An amorphous apatite layer is thought to be advantageous from the biological standpoint since the hydroxyapatite found in human bone is also amorphous.

5. Conclusions

This work characterized the physical and chemical properties of Y:TZP/TiO_2 bioceramic specimens that were covered with a calcium phosphate layer. It was demonstrated that the calcium phosphate layer was crystalline for specimens with 30% of TiO_2 and amorphous for specimens with 0 and 10% of TiO_2. Chemical analysis indicated that this layer was composed of type A carbonate apatite, which is expected to deliver good bioactivity since it is also found in bone mineral. Among the materials tested, the composite with 10% of TiO_2 showed the highest density and should be further explored as an option for dental implants.

Acknowledgments

This investigation was financial supported by FAPESP, CNPq and UFABC.

The authors thank Laboratório de Microscopia do Centro de Ciência e Tecnologia de Materiais do Instituto de Pesquisas Energéticas e Nucleares for their support with microstructure analyses and da Silva AC for help in DRITF experiments.

REFERENCES

[1] Shibli JA, Grassi S, de Figueiredo LC, Feres M, Marcantonio Jr E, Iezzi G, et al. Influence of implant surface topography on early osseointegration: a histological study in human jaws. Journal of Biomedical Materials Research Part B: Applied Biomaterials 2007;80:377–85.

[2] Shibli JA, Grassi S, de Figueiredo LC, Feres M, Iezzi G, Piattelli A. Human peri-implant bone response to turned and oxidized titanium implants inserted and retrieved after 2 months. Implant Dentistry 2007;16:252–9.

[3] Egusa H, Ko N, Shimazu T, Yatani H. Suspected association of an allergic reaction with titanium dental implants: a clinical report. Journal of Prosthetic Dentistry 2008;100:344–7.

[4] Warashina H, Sakano S, Kitamura S, Yamauchi K-I, Yamaguchi J, Ishiguro N, et al. Biological reaction to alumina, zirconia, titanium and polyethylene particles implanted onto murine calvaria. Biomaterials 2003;24:3655–61.

[5] Ko H-C, Han J-S, Bachle Ma, Jang J-H, Shin S-W, Kim D-J. Initial osteoblast-like cell response to pure titanium and zirconia/alumina ceramics. Dental Materials 2007;23:1349–55.

[6] Chevalier J. What future for zirconia as a biomaterial? Biomaterials 2006;27:535–43.

[7] Lughi V, Sergo V. Low temperature degradation aging of zirconia: a critical review of the relevant aspects in dentistry. Dental Materials 2010;26:807–20.

[8] Scarano A, Di Carlo F, Quaranta M, Piattelli A. Bone response to zirconia ceramic implants: an experimental study in rabbits. Journal of Oral Implantology 2003;29:8–12.

[9] Piconi C, Maccauro G, Muratori F, Brach Del Prever E. Alumina and zirconia ceramics in hip replacements. Journal of Applied Biomaterials and Biomechanics 2003;1:19–32.

[10] Hao L, Ma DR, Lawrence J, Zhu X. Enhancing osteoblast functions on a magnesia partially stabilized zirconia bioceramic by means of laser irradiation. Materials Science and Engineering 2005;25:496–502.

[11] Wenz HJ, Bartsch J, Wolfart S, Kern M. Osseointegration and clinical success of zirconia dental implants: a systematic review. International Journal of Prosthodontics 2008;21:27–36.

[12] Agins HJ, Alcock NW, Bansal M, Salvati EA, Wilson Jr PD, Pellicci PM, et al. Metallic wear in failed titanium-alloy total hip replacements. A histological and quantitative analysis. Journal of Bone and Joint Surgery 1988;70:347–56.

[13] Pelaez-Vargasa A, Gallego-Perez D, Magallanes-Perdomo M, Fernandes MH, Hansford DJ, DeAza AH, et al. Isotropic micropatterned silica coatings on zirconia induce guided cell growth for dental implants. Dental Materials 2011;27:581–9.

[14] Kim HW, Georgiou G, Knowles JC, Koh YH, Kim HE. Calcium phosphates and glass composite coatings on zirconia for enhanced biocompatibility. Biomaterials 2004;25:4203–13.

[15] Marchi J, Ussui V, Delfino CS, Bressiani AHA, Marques MM. Analysis in vitro of the cytotoxicity of potential implant materials. I: Zirconia–titania sintered ceramics. Journal of Biomedical Materials Research Part B: Applied Biomaterials 2010;94B:305–11.

[16] Ananta S, Tipakontitikul R, Tunkarisi T. Synthesis, formation and characterization of zirconium titanate (ZT) powders. Materials Letters 2003;57:2637–42.

[17] Bianco A, Paci M, Freer R. Zirconium titanate: from polymeric precursors to bulk ceramic. Journal of the European Ceramic Society 1998;18:1235–43.

[18] Kasuga T, Kondo H, Nogami M. Apatite formation on TiO_2 in simulated body fluid. Journal of Crystal Growth 2002;235:235–340.

[19] Uchida M, Kim H-M, Kokubo T, Nakamura T. Apatite-forming ability of titania gels with different structures. In: Ohgushi H, Hastings GW, Yoshikawa T, editors. Bioceramics. Singapore: World Scientific Publishing; 1999. p. 149–52.

[20] Silva CCG, Rigo ECS, Marchi J, Bressiani AHA, Bressiani JC. Study of apatite deposition on several silicon nitride substrates. Materials Research 2008;11:47–50.

[21] Pierri JJ, Roslindo EB, Tomasi RO, Pallone EMJA, Rigo ECS. Alumina/zirconia composite coated by biomimetic method. Journal of Non-Crystalline Solids 2006;352:5279–83.
[22] Jonasova L, Muller FA, Helebrant A, Strnad J, Grei P. Hydroxyapatite formation on alkali-treated titanium with different content of Na^+ in the surface layer. Biomaterials 2002;3:3095–101.
[23] Rigo ECS, Santos LA, Carrodeguas RG, Boschi AO. Bonelike apatite coating on $Ti_6A_{l4}V$: novel nucleation process using sodium silicate solution. Materials Science Forum 2003;416–418:658–62.
[24] Ussui V, Leitão F, Yamagata C, Menezes CAB, Lazar DRR, Paschoal JOA. Synthesis of ZrO_2 based ceramics for applications in SOFC. Materials Science Forum 2003;416–418:681–7.
[25] Chiang YM. Physical ceramics. In: Principles for ceramic science and engineering. New York: John Wiley & Sons; 1997.
[26] Haynes WM. CRC handbook of chemistry and physics. Standard reference data. USA: National Institute of Standards and Technology; 2011. p. 92.
[27] Picart C. Polyelectrolyte multilayer films: from physico-chemical properties to the control of cellular processes. Current Medicinal Chemistry 2008;15:685–97.
[28] Tengvall P, Lündstrom I. Physico chemical considerations of titanium as a biomaterial. Clinical Materials 1992;9:115–34.
[29] Marchi J, Greil P, Bressiani JC, Bressiani AHA, Muller F. Influence of synthesis conditions on the characteristics of biphasic calcium phosphate powders. International Journal of Applied Ceramic Technology 2009;6:60–71.
[30] Merkus HG. Particle size measurements. Fundamentals, practice, quality. particle technology series, vol. 17. Heidelberg: Springer; 2009.
[31] Kokubo T. Apatite formation on surfaces of ceramics, metals and polymers in body environment. Biomaterials 1991;12:155–63.
[32] Rey C, Renugopalakrishnan V, Collins B, Glimcher MJ. Fourier transform infrared spectroscopic study of the carbonate ions in bone mineral during aging. Calcified Tissue International 1991;49:251–8.
[33] Rey C, Renugopalakrishnan V, Shimizu M, Collins B, Glimcher MJ. A resolution-enhanced Fourier transform infrared spectroscopic study of the environment of the CO_3^{2-} ion in the mineral phase of enamel during its formation and maturation. Calcified Tissue International 1991;49:259–68.
[34] Gibson IR, Bonfield W. Novel synthesis and characterization of an AB-type carbonate-substituted hydroxyapatite. Journal of Biomedical Materials Research 2002;59:697–708.
[35] Rey C, Collins B, Goehl T, Dickson IR, Glimcher MJ. The carbonate environment in bone mineral: a resolution-enhanced Fourier transform infrared spectroscopy study. Calcified Tissue International 1989;45:157–64.